

Simultaneous intensive photometry and high resolution spectroscopy of δ Scuti stars

III. Mode identifications and physical calibrations in HD 2724*

M. Bossi¹, L. Mantegazza¹, and N.S. Nuñez^{1,2}

¹ Osservatorio Astronomico di Brera, Via Bianchi 46, I-23807 Merate LC, Italy

² Observatorio Astronómico P. Buenaventura Suarez, C.C. 1129, Asunción, Paraguay

Received 25 March 1998 / Accepted 25 May 1998

Abstract. On the basis of our new simultaneous photometry and spectroscopy (885 *uvby* differential measurements in 11 nights and 154 spectrograms of the FeII λ 4508 region in 5 nights), we can detect 12 probable periodicities in the variability pattern of this star, determining the frequencies of 7 without any ambiguity. Through a direct fit of pulsational models to our data, we estimate the inclination of rotational axis to be about 50° and get a reliable identification of 4 modes as well as useful bits of information about the others: no retrograde mode is visible, whereas the star seems to show a certain preference for purely sectorial prograde oscillations. Finally, the attribution of our lowest frequency to the radial fundamental pulsation allows a new calibration of physical parameters. In particular, the gravity can be determined with unusual accuracy and the luminosity evaluation becomes more consistent with the Hipparcos astrometry.

Key words: methods: data analysis – stars: fundamental parameters – stars: individual: HD 2724 – stars: oscillations – δ Sct

1. Introduction

The serendipitous discovery of HD 2724 as a variable star is due to Reipurth (1981), which chose it as one of the comparison objects for his differential photometry of the eclipsing binary AG Phe. The author identified HD 2724 as a probable δ Scuti star and guessed a tentative period of $0^d.174$ (i.e. a frequency of 5.75 d^{-1}). Lampens (1992) met this periodicity again analysing her excellent sequences of absolute measurement obtained at La Silla in 1984–85 by means of the UBVB₁B₂V₁G Geneva photometer. Lampens' analysis shows multiperiodic variations which are typical of the δ Scuti light curves: besides the above mentioned frequency, she identified unambiguously another component at $\sim 7.38 \text{ d}^{-1}$ and suggested $\sim 6.50 \text{ d}^{-1}$ and $\sim 4.34 \text{ d}^{-1}$ as two additional candidate frequencies.

Send offprint requests to: M. Bossi, (bossi@merate.mi.astro.it)

* This work is based on observations performed at the European Southern Observatory (ESO), La Silla, Chile.

HD 2724 is classified as an F2 III star in Hoffleit and Jaschek (1982). Lampens (1992) gets from her photometry $T_{eff} = 7180^\circ\text{K}$ and $M_V = 0.93$. Physical parameters can be evaluated also by using the *uvby* β colours published by Hauck & Mermilliod (1990). Moon's & Dworetzky's (1985) grids lead us to estimate T_{eff} and $\log g$ at 7280°K and 3.56 respectively, while Villa & Breger (1998) obtain from their still unpublished calibration, based on Canuto's & Mazzitelli's (1991) models and performed using dereddened indices, $T_{eff} = 7216^\circ\text{K}$ and $\log g = 3.64$. As to the absolute magnitude, Crawford's (1979) calibration yields $M_V = 1.12$, $E(b-y) = 0.014$ and therefore $A_V = 0.060$. Nevertheless, our photometric evaluations of luminosity are now to be revised owing to new astrometric data: in the Hipparcos Satellite General Catalogue (ESA, 1997), this object (HIC 2388) appears with a parallax $\pi = 7.77 \pm .72 \text{ mas}$, which, taking account of the above assessed interstellar extinction, corresponds to an absolute magnitude $M_V = 0.57 \pm .20$. In principle, pulsational masses could help us to adjust these calibrations. It would entail, however, a thorough knowledge of pulsational states, which today might be achieved only by combining photometry and spectroscopy in a synergetic approach (see e.g. Bossi et al., 1994, or Mantegazza et al., 1998).

In order to exploit the complementarity between photometry and spectroscopy in studying dynamical processes like stellar pulsations, we are performing for many years simultaneous observational campaigns of δ Scuti stars through both these techniques (Mantegazza et al., 1994; Mantegazza & Poretti, 1996). The present work on HD 2724 falls within this frame.

2. Observations and data processing

Both our photometry and spectroscopy have been performed at the ESO Observatory (La Silla, Chile) in September 1993.

Our photometric data consist of 885 *uvby* differential measurements obtained through the Danish 0.5 m telescope and spread over 11 almost consecutive nights with a baseline of ~ 11 days, the total useful observation time amounted to ~ 90 hours. As comparison stars we employed HD 3136, HD 1683 and HD 1856. All the magnitude and colour differences are given with respect to the reference star HD 3136: our large set

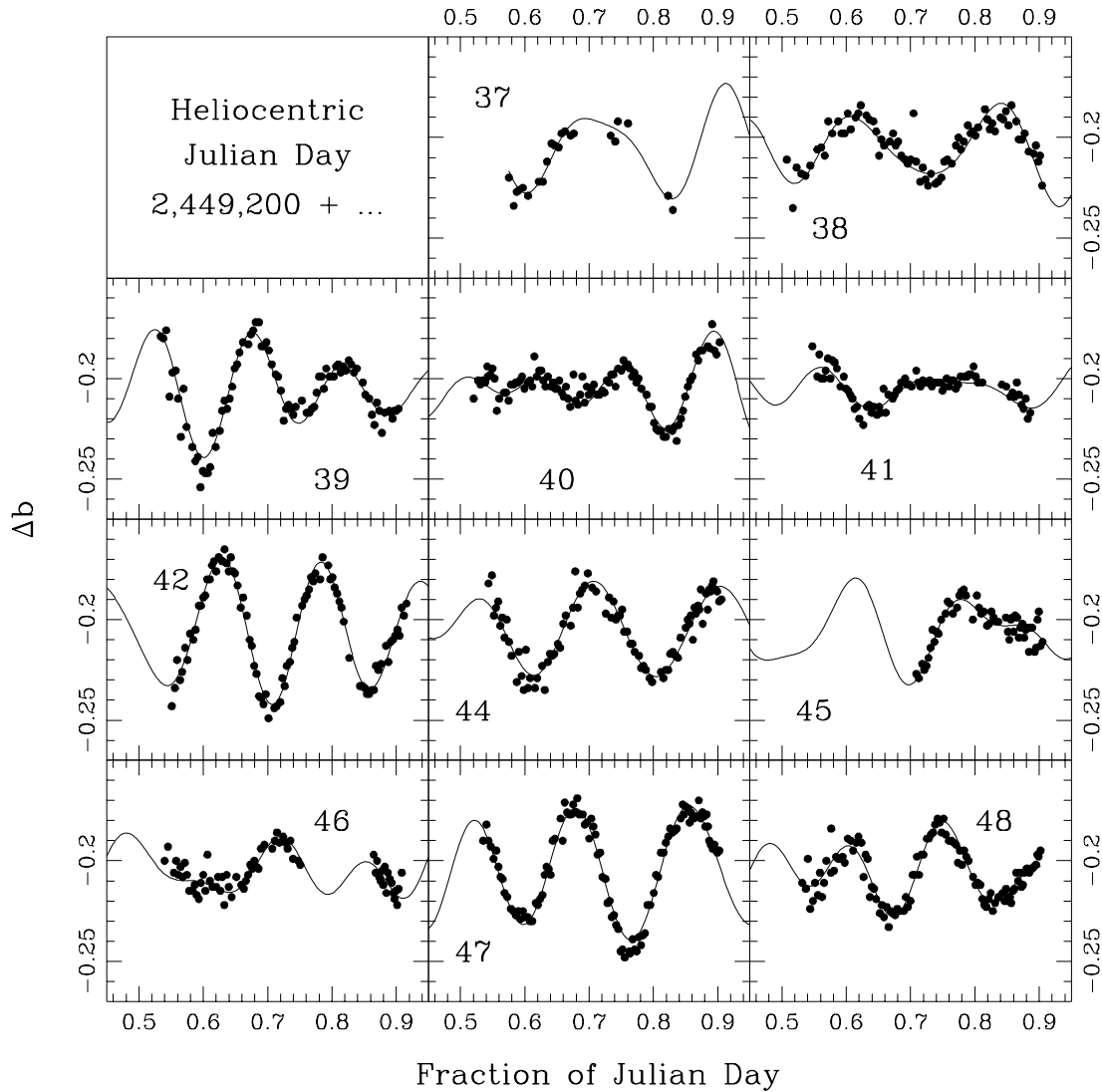


Fig. 1. Δb light curve of HD 2724 (dots) compared with its best fitting 10 sinusoid model (solid line) as shown in Table 2; the luminosity grows upward.

of data allowed us to do it by shifting all the comparison objects to the same fictitious magnitudes with great accuracy. Considering the size of our observational field (HD 1683 is about 4° to the NW of HD 3136), the data have been processed using the technique developed by Poretti and Zerbi (1993) in order to deal with the variations in extinction coefficients during each night.

The basic statistical parameters which characterize the resulting light curves of HD 2724 and their reliability are presented in Table 1, where the white noise content of each time series has been evaluated from the root-mean-square difference between closely consecutive data. In every light-band, the standard deviations of the HD 1683 - HD 3136 (Ck1) and HD 1856 - HD 3136 (Ck2) curves, indistinguishable from the corresponding white noises, assure the stability of our comparison stars.

As expected in a δ Scuti star, we got the best signal-to-noise ratios in the Δv and Δb series. The Δb light curve is displayed in Fig. 1 (the dots correspond to individual measurements).

Table 1. Statistical parameters characterizing our differential light curves of HD 2724 and their reliability.

	Δu	Δv	Δb	Δy
Standard deviation (mmag)	16.8	18.9	15.9	13.6
White noise (mmag)	9.2	5.9	4.7	4.9
S/N ratio (dB)	4	10	10	8
Ck1 Stand. Dev. (mmag)	8.9	5.4	4.9	5.4
Ck2 Stand. Dev. (mmag)	8.0	5.3	5.0	5.0

Simultaneously with our photometric measurements, we performed spectroscopic observations using the Coudé Echelle Spectrograph (CES) attached to the Coudé Auxiliary Telescope (CAT) and equipped with a CCD detector. The adopted config-

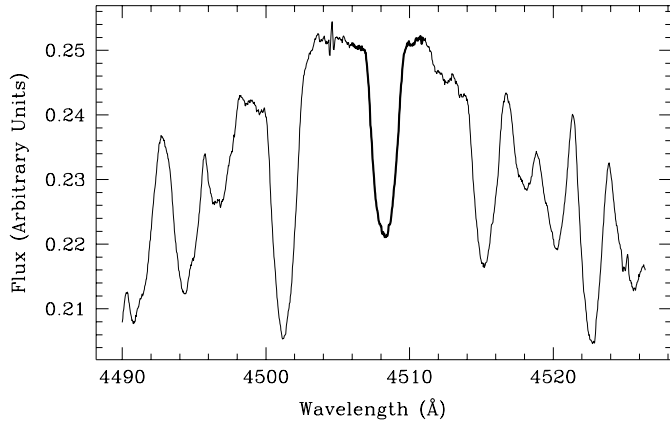


Fig. 2. The average of our 154 spectrograms; the FeII line at ~ 4508 Å has been prominently displayed.

uration and the exposure times, which varied between 10 and 15 minutes, gave a wavelength resolution of ~ 0.075 Å with a sampling of ~ 0.036 Å in the range 4490–4526 Å with an average signal-to-noise ratio at the continuum level of ~ 47 dB (i.e., in a linear scale, a ratio of 1 to ~ 233 between the noise standard deviation and the continuum flux). The resulting 154 spectrograms, distributed over 5 consecutive nights with a total useful observing time of about 34 hours, have been processed using the MIDAS package developed by the ESO.

The mean spectrum displayed in Fig. 2 shows that the star is a moderately fast rotator. In the observed region, the blending of adjacent features spares the sole FeII line at 4508.29 Å: only this line borders on stretches of spectral continuum enough to allow its stable normalization.

The average FeII $\lambda 4508$ line profile resulting from the normalization to the continuum flux is compared in the top of Fig. 3 with its best fitting synthetic profile obtained convolving together the instrumental profile, a gaussian intrinsic profile corresponding to an atomic iron gas at $7,200$ K and a rotational profile. This procedure yields an estimate of the Doppler broadening $v \sin i = 82$ km s $^{-1}$ with an uncertainty of the order of 2 km s $^{-1}$.

In the bottom of the same Fig. 3 we present, as a function of the wavelength, the variance of the sequences consisting of the successive flux values (normalized to the stellar continuum) registered at each pixel. These variances have been previously purified of the white noise contributions, which have been evaluated pixel by pixel determining, like we did in the analysis of our photometric series, the root-mean-square differences between closely consecutive data. Apparently, the star shows a considerable spectral variability: the height of the main variance peak indicates variations of flux whose standard deviation exceeds the 0.8% of the continuum level.

3. Frequency analysis

The frequency analysis of our photometric sequences has been performed both by using the CLEAN algorithm (Roberts et al., 1987) and through the least-square sine-fitting technique (Van-

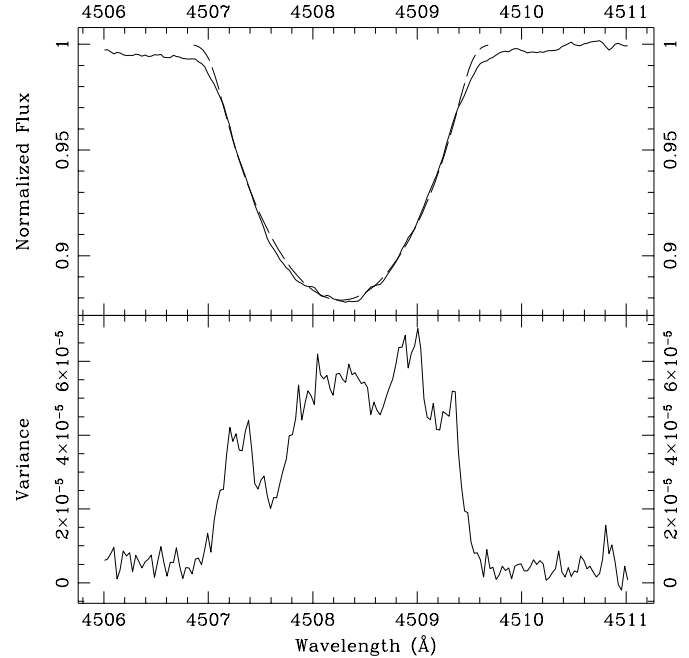


Fig. 3. The FeII line region at ~ 4508 Å: average of our 154 spectrograms normalized to the continuum flux (top, solid line); the best fitting synthetic profile corresponding to $v \sin i = 82$ km s $^{-1}$ (top, dashed line); variance of the signal as a function of the wavelength (bottom).

icek, 1971; Mantegazza et al., 1995). At each step of Vanicek's procedure, the outcomes have been systematically adjusted by means of simultaneous nonlinear least squares fits. These methods made us able to detect the presence of at least 10 periodic components in our light curves. An outline of the best fitting 10 frequency model for the Δb curve is presented in Table 2. The fitting curve (solid line) can be visually compared with the measurements (dots) in Fig. 1. Also a comparison between the root-mean-square residual (4.9 mmag) and the corresponding white noise (4.7 mmag) shows this solution to represent the light variations quite reasonably. Nevertheless, we are allowed to consider only 7 frequencies as completely reliable: if we examine different curves (Δy , Δv or Δu) and/or if we model them with a different number of periodicities (9 or 11), we can improve some fits replacing ν_2 , ν_4 and/or ν_{10} with values at a distance of ~ 1 d $^{-1}$. We have to point out that ν_2 and ν_4 are close to the resolution limit respectively from ν_1 and ν_5 , i.e. from the first and the third strongest components of the observed variability. Obviously, this fact entangles our frequency spectra hindering us in the identification of the significant peaks. On the other hand, no doubt either these periodicities or the alternative ones at ± 1 d $^{-1}$ are present in our signals: tests performed using synthetic data (Bossi & Nuñez, in preparation) made us sure that our procedures permit frequency resolutions substantially better than the conventional ones. Anyway, in consequence of these ambiguities, we must regard the errors presented in Table 2 as lower bounds. They have been determined by means of the standard statistical approach assuming the observed variability to consist just of the 10 considered sinusoids and white noise:

Table 2. The best fitting 10 sinusoid model of the Δb light curve; the phases are referred to $t_0 = \text{H.J.D. } 2,449,243.6950$.

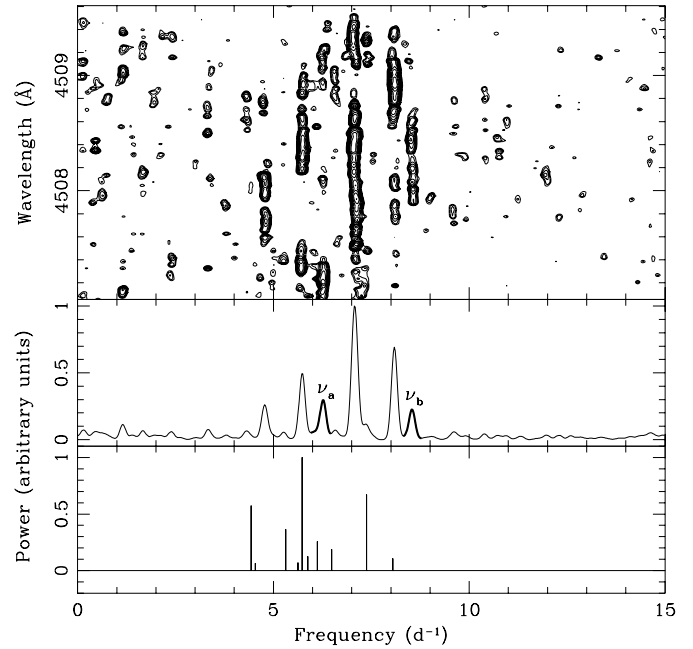
Comp.	Frequency (d^{-1})	Amplitude (mmag)	Phase (rad)
ν_1	$4.430 \pm .002$	$8.4 \pm .3$	$-1.14 \pm .04$
ν_2	$4.536 \pm .008$	$2.8 \pm .3$	$3.06 \pm .11$
ν_3	$5.311 \pm .002$	$6.7 \pm .3$	$0.21 \pm .04$
ν_4	$5.629 \pm .007$	$2.9 \pm .3$	$-3.04 \pm .11$
ν_5	$5.736 \pm .001$	$11.1 \pm .3$	$2.28 \pm .03$
ν_6	$5.877 \pm .003$	$3.9 \pm .3$	$-2.25 \pm .08$
ν_7	$6.123 \pm .002$	$5.6 \pm .3$	$-0.78 \pm .05$
ν_8	$6.488 \pm .003$	$4.8 \pm .3$	$1.87 \pm .06$
ν_9	$7.382 \pm .001$	$9.1 \pm .3$	$-0.34 \pm .03$
ν_{10}	$8.049 \pm .003$	$3.6 \pm .3$	$-1.64 \pm .07$

the replacement of one of these components with an alternative periodicity results in affecting the determination of all the other parameters. Another series of tests showed us, for example, how a prudent evaluation of the frequency uncertainties, which should take aliasing phenomena into account, would increase the error bars associated with unambiguous components to $\sim 0.01 \text{ d}^{-1}$.

Reipurth's (1981) periodicity is recognizable as ν_5 and also the frequencies indicated by Lampens (1992) with the surprising number of 5 decimal places lie close to ν_1 , ν_5 , ν_8 and ν_9 . In order to check if the pulsational status of this star is stable in time scales of years, Lampens' measurements might deserve a further analysis. In fact, those data permitted the detection of four substantially correct frequencies in spite of their unfortunate distribution and in spite of the rough prewhitening technique adopted by the author: if we resort to this procedure in the presence of complex multiperiodic behaviours, sensible fit errors accumulate step by step in the successively analysed residuals, eventually leading us on the wrong track.

The analysis of photometric data is not bound to exhaust the search for detectable pulsations: the presence of high ℓ -degree modes affects the spectral line profiles, especially if broadened by an high projected rotational velocity, more than the observed luminosity. Therefore, a period analysis of the $\text{FeII}\lambda 4508$ profile variations has been performed pixel by pixel using again both Vanicek's (1971) method (see also Mantegazza, 1997) and the CLEAN algorithm. The top panel of Fig. 4 shows the resulting CLEAN spectrum as a function of the wavelength; moving to the bottom, we meet the corresponding mean spectrum and finally we can compare it with a photometric power spectrum drawn according to the model of Table 2. Vanicek's outcomes reveal the presence of few more photometric frequencies in our spectroscopic series, but they are not very practical for graphic presentation: each detected component would need its figure.

The inadequacy of our spectroscopic data window is apparent: a) ν_5 and ν_{10} switch between two alternative frequency values at a distance of 1 d^{-1} changing the wavelength, i.e. the

**Fig. 4.** From the top to the bottom: the CLEAN spectrum of the flux series describing pixel by pixel the evolution of the $\text{FeII}\lambda 4508$ line profile shown as a function of the wavelength, the corresponding mean spectrum and the photometric power spectrum which results from the model of Table 2.

phases of the corresponding oscillations; b) the spectral resolution would not be enough for separating frequencies close to each other like ν_4 , ν_5 and ν_6 . Anyway, as it was only to be expected, pulsations manifest themselves in photometric and spectroscopic variations with independent intensities: ν_{10} , which in Table 2 shows the third last amplitude, is beyond all doubt the dominant spectroscopic periodicity. Besides the above quoted ν_{10} and ν_5 , also the photometric frequency ν_9 can be immediately recognized in the bump on the right of the main peak of our CLEAN mean spectrum. The components at ~ 6.27 (ν_a) and $\sim 8.55 \text{ d}^{-1}$ (ν_b), prominently displayed in the same panel of Fig. 4 and invisible in the light curves, are likely to correspond to real periodicities too: they do not disappear even assuming ν_7 and ν_8 as known constituents in Vanicek's analysis. Finally, Vanicek's (1971) approach allows us, adding ν_3 and ν_8 , to complete our set of spectroscopic frequencies.

4. Mode identification

The technique developed by Garrido et al. (1990) in order to discriminate between radial and low ℓ -degree non-radial pulsations in δ Scuti stars following Dziembowski (1977) and Watson (1988) could help us, in principle, with the characterization of our 10 photometric modes. Nevertheless, phase uncertainties comparable with the expected lags hinder us in quarrying in our Strömgren curves for useful bits of information. Fig. 5 displays e.g. the phase shifts between the v and the y variations shown by each of these components: we cannot get from this kind of diagram much more than a marginal evidence supporting the

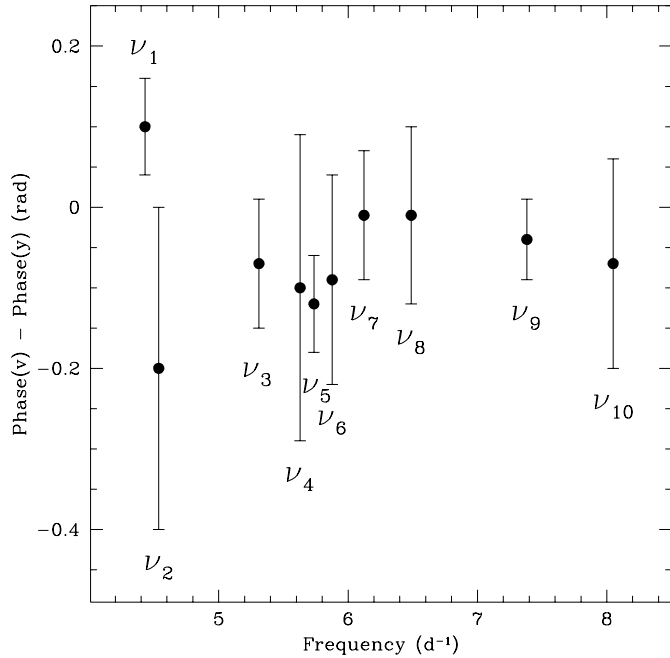


Fig. 5. Phase shifts between v and y shown by the periodic components of our light curves.

radial character of ν_1 suggested also by its merely photometric relevance. On the other hand, the absence of ν_a and ν_b in our photometric signal implies relatively high ℓ -values for them.

At this point, we could not go any farther without resorting to some line profile analysis. The most common tools to perform such computer-limited task in reasonable calculating times are currently the moment method proposed by Balona (1987) and the two-dimensional Fourier analysis combined with the Doppler imaging by Kennelly et al. (1992). The last approach is in principle the most suitable one for the study of rapidly rotating objects like HD 2724: a dominant Doppler broadening makes the spectral lines useful as one-dimensional maps of the stellar surfaces. This ought to permit at least the immediate determination of the m -numbers. Nevertheless, as shown by Telting & Schrijvers (1995), to rely mechanically on this technique is dangerous: under certain conditions ($|m| < \ell$; $i \ll 90^\circ$), its unthinking use leads us to overestimate $|m|$. On the other hand, Balona's (1987) procedure is based on a series of strong simplifications perhaps today less and less necessary due to the continuous advance of computer technology.

For those reasons, at Balona's (1997) suggestion, we nerved ourselves to perform a direct fit of pulsational models to our line profile variations taking also the photometric measurements into account.

1. The first step was a simultaneous least-square fit performed pixel by pixel adjusting the sum of a constant parameter plus 7 sinusoids to each sequence of normalized fluxes. We assumed the frequencies of the periodic terms to be the ones singled out in the preceding section as relevant to the spectroscopic variability: ν_3 , ν_5 , ν_8 , ν_9 , ν_{10} , ν_a and ν_b . The set of constant parameters describes the unperturbed line pro-

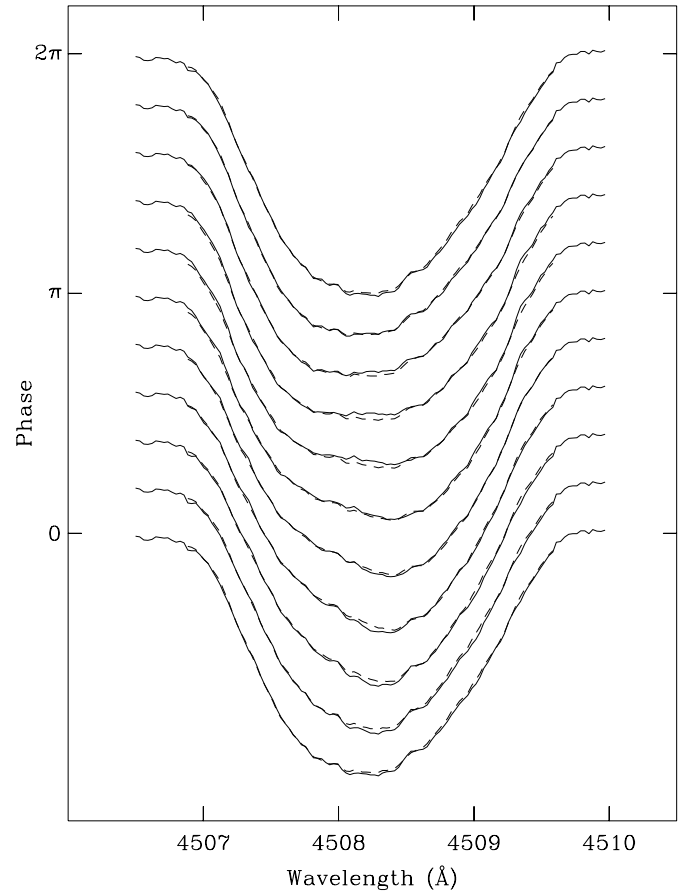


Fig. 6. The component of the line profile variability corresponding to the frequency $\nu_5 \simeq 5.74 \text{ d}^{-1}$ (solid lines), compared with the best fitting synthetic model (dashed lines), corresponding to $\ell=2$, $m=-2$, $i=50^\circ$.

file, while each group of sinusoids draws the corresponding periodic component of the profile variations. The pattern of the main photometric component ν_5 ($\sim 5.74 \text{ d}^{-1}$), quarried out of our data by means of this procedure, is shown for example in Fig. 6 (solid lines).

2. We assumed as fixed input parameters a r.m.s. intrinsic line width $W_i = 11.4 \text{ Km s}^{-1}$, a Doppler broadening $v \sin i = 81.7 \text{ Km s}^{-1}$ and a limb darkening coefficient $u_{\lambda 4509} = 0.7$: the values of W_i and of the projected rotational velocity resulted from a simultaneous non-linear least-square fit performed on the unperturbed profile assuming a gaussian intrinsic line shape; for the limb darkening see e.g. Díaz-Cordovés et al. (1995). As regards the inclination i of the rotational axis, we scanned the range 30° - 90° with a resolution of 7.5° ($i \leq 22.5^\circ$ would entail an equatorial velocity of at least 215 Km s^{-1}).
3. Each of the 7 above quoted variability components has been described putting 10 instantaneous line profiles, with phase intervals of $\pi/5$ like in Fig. 6, together with the corresponding photometric pattern defined in Table 2. Obviously, the photometric amplitude assigned to the purely spectroscopic components ν_a and ν_b was zero. Then, 10 synthetic pro-

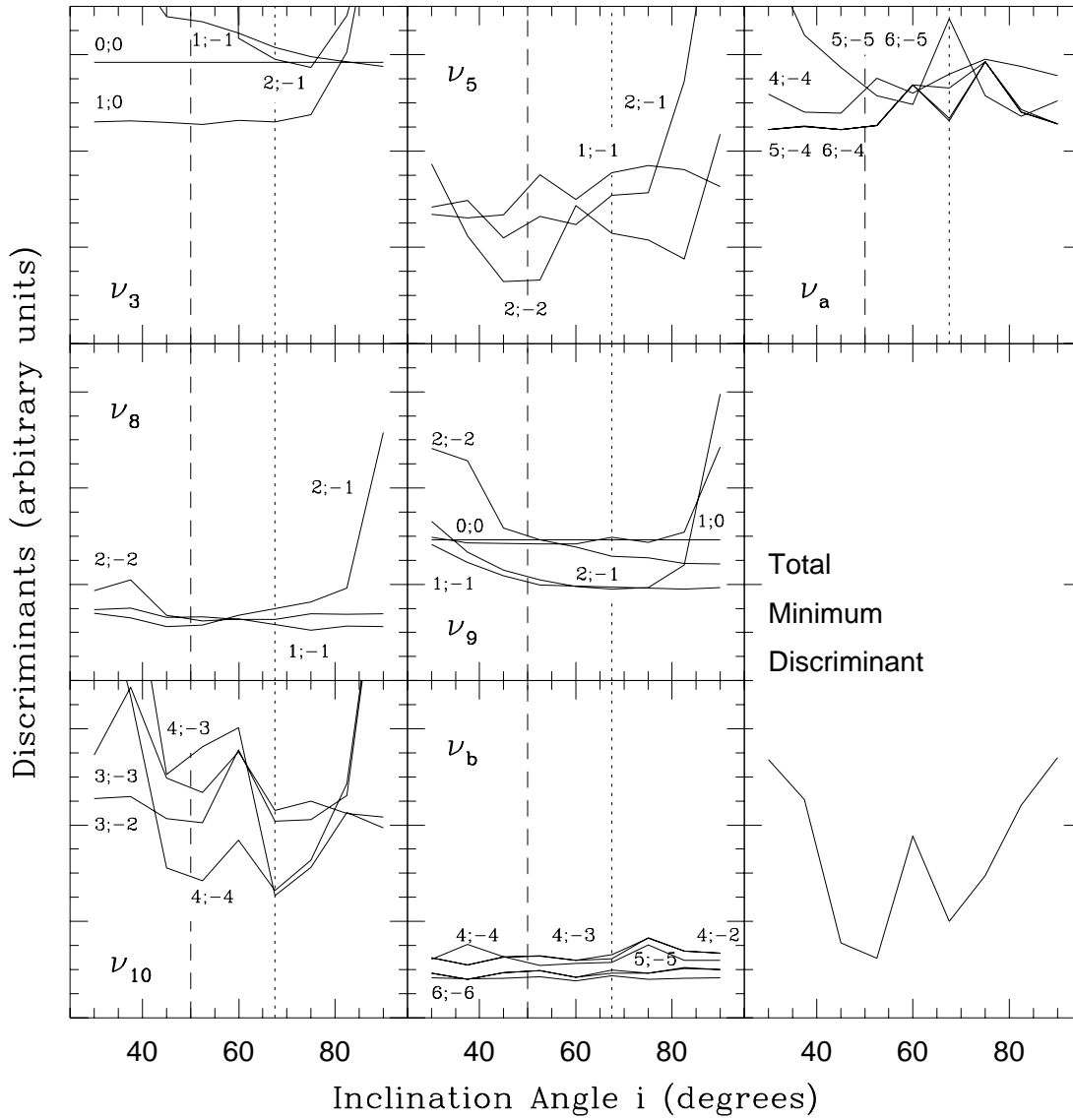


Fig. 7. Minimum discriminant values, corresponding to the best fitting candidate couples ($\ell; m$), shown as functions of the inclination angle for each frequency which we could detect in the spectral variability. The panel visible low on the right shows, in the same scale and again as a function of i , the sum of the 7 minimum discriminants.

files and a synthetic light curve have been adjusted to these data by means of a non-linear least-square technique for each possible candidate mode, i.e. for each plausible couple of ($\ell; m$) numbers, and for each explored value of the i parameter. Both the spectroscopic and photometric models have been produced through the LNPROF code, kindly put at our disposal by L.A. Balona. Balona's algorithm uses a first order expansion in the ratio Ω/ω of the rotational frequency to the pulsational one: a comparison of $\Omega \approx 0.5/\sin i \text{ d}^{-1}$ to our 7 scrutinized frequencies makes this approximation quite reasonable. Finally, assuming the presence of p modes and operating in adiabatic approximation, we could link the horizontal displacement velocity V_h with the vertical one V_r through the relation $V_h \approx 74.4 Q^2 V_r$. Thus, only 4 free parameters remained to be determined for each

fixed ℓ , m and i : the amplitudes and phases of the luminance modulation on the stellar surface and of V_r . These parameters have been adjusted combining the mean-square differences between observational and synthetic models in one discriminant which assigns equal weights to photometry and spectroscopy, and minimizing it through the iterative downhill simplex method (Press et al., 1992). In Fig. 6, for example, we can compare the best fitting synthetic profiles which describe the component ν_5 of the spectral variability (dashed lines) to the observational ones (solid lines). The resulting discriminant values are shown in Fig. 7 for each frequency and for the best fitting candidate couples ($\ell; m$) as functions of the inclination angle.

4. In order to get information about the plausible inclination of the rotational axis, taking our bearing among the pulsational

modes, we computed, again as a function of i , the sum of the minimum discriminants corresponding to the 7 frequencies which we could detect in the spectral variability (see the panel visible low on the right in the same figure).

The inclination angle i results likely to be close to 50° , even if an alternative value between 65° and 70° cannot be ruled out. In Fig. 7, these angles are indicated by the vertical dashed line and by the dotted one respectively: it is easy to notice how the choice of the first value, besides minimizing the r.m.s. residual, to some extent disentangles the mode identification. As regards the pulsational modes, our information, considering also the photometric phase shifts, is summarized in Table 3. Despite the incompleteness of these results, an item deserves a certain interest: we detected no retrograde perturbation. No way it can be a simple observational bias due to the fast rotation of HD 2724: the sign of m is defined by our code in a co-rotating reference frame. If we might hazard a second more uncertain guess, we would also say this class of stars prefers, among the prograde non-radial pulsations, the purely sectorial ones.

5. Physical parameters

The representative points of HD 2724 in the plane ($\log g$; T_{eff}) which correspond to the calibrations of Moon & Dworetzky (1985) and of Villa & Breger (1998) are shown in Fig. 8 respectively by the black dot and by the open circle. In the same figure, assuming Hipparcos' parallax, the solid line indicates the gravity-temperature combinations which associate our lowest frequency ν_1 with a pulsational constant $Q = Q_0 = 0^d.033$, i.e., according to Fitch (1981), with the fundamental radial pulsation. Finally, the identification of ν_1 as a g_1 mode with $\ell = 2$ and $Q = 0^d.051$ (cf. again Fitch, 1981) corresponds in the figure to the dashed line. We have no reasonable alternative but these two possible Q values. For one thing, in fact, the identification of ν_1 as an high- ℓ g -mode is very improbable: considering its photometric amplitude, an high degree non-radial oscillation would be easily detected in our spectrograms. For another thing, both radial overtones and non-radial p-modes would entail unrealistic pulsational constants $Q < Q_0$.

Combined with the evolutionary models of Shaller et al. (1992), the association of ν_1 with $Q = 0^d.051$ does not allow us to reconcile photometry with astrometry. This choice, characterizing our object as a $2 M_\odot$ star with $T_{eff} = 7200^\circ\text{K}$, $\log g = 3.67$ and $M_V = 1.1$, would lead us back to Crawford's (1979) magnitude calibration, at a $\sim 3\sigma$ distance from Hipparcos' one.

Therefore, we can add the astrometric evidence to our previous indications (cf. the last section) in support of the radial hypothesis, we can identify ν_1 as the fundamental mode and have a try assuming only an effective temperature of $7200 \pm 100^\circ\text{K}$ and a pulsational constant $Q_0 = 0^d.033$ with a theoretical uncertainty of the order of $0^d.001$ (Fitch, 1981). The evolutionary tracks of Schaller et al. (1992) can be easily translated, like in Fig. 9, from the plane ($\log(L/L_\odot)$; $\log T_{eff}$) into the plane (M_{bol} ; ν_0), where ν_0 is the frequency of the fundamental mode determined assuming $Q_0 = 0^d.033$. The instants that the stars, following

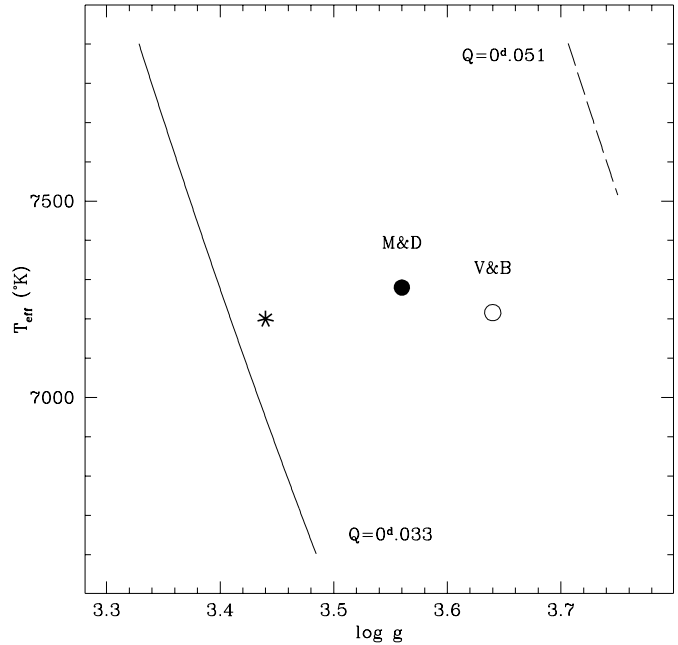


Fig. 8. Representative points of HD 2724 in the plane ($\log g$; T_{eff}) according to the calibration of Moon & Dworetzky (black spot), to Villa's & Breger's (1998) method (open circle) and to the results shown in the present work (asterisk). Assuming Hipparcos' parallax, the solid line corresponds to the identification of ν_1 as the fundamental pulsation, the dashed one as a g_1 mode with $\ell = 2$.

downwards their evolutionary paths (solid lines), reach an effective temperature $T_{eff} = 7200^\circ\text{K}$ are indicated by dots: for $M = 1.7 M_\odot$ it occurs outside the panel, while a star with $M = 1.5 M_\odot$ keeps always below this temperature. Finally, an horizontal dashed line corresponds to our frequency ν_1 . This picture allows us to assign to HD 2724, which we are apparently observing during its expansion immediately after the exhaustion of the hydrogen burning, a mass of about $2.25 M_\odot$, a bolometric absolute magnitude not far from 0.4 and a surface gravity $\log g \simeq 3.44$. The asterisks in Fig. 8 and Fig. 9 show the corresponding representative points respectively in the plane ($\log g$; T_{eff}) and (M_{bol} ; ν_0). In Fig. 9, according to Hipparcos parallax, we ought to locate it in the position indicated by the open circle with horizontal error bar: since the absolute magnitude value was not among our assumptions, neither the closeness of these points nor, in Fig. 8, the adjacency of the star to the line corresponding to Q_0 were to be taken for granted a priori.

The consistency of these results leads us to summarize the corresponding physical picture in Table 4. The asymmetrical uncertainty assigned to the absolute bolometric magnitude takes both our model and the above quoted astrometric constraint into account.

The rotational frequency appears even lower than previously expected (cf. Sect. 4, point 3), making our linear expansion in Ω/ω wholly legitimate *a posteriori*. The value of Ω shown in Table 4 has been used for evaluating the proper pulsational frequencies referred to a co-rotating frame presented in the third column of Table 3. If correctly identified, the two components

Table 3. Mode identification obtained combining photometric and spectroscopic information and accepting the most probable inclination $i \simeq 50^\circ$. The third column shows the corresponding frequencies in a co-rotating reference frame obtained assuming a rotational frequency $\Omega = 0.45 \pm 0.03 \text{ d}^{-1}$.

Component	Plausible $\ell; m$	Proper frequency (d^{-1})
ν_1	0;0	4.43 ± 0.01
ν_2	non-radial mode	
ν_3	1;0	5.31 ± 0.01
ν_4	non-radial mode	
ν_5	2;-2	4.84 ± 0.07
ν_6	0;0?	$5.88 \pm 0.01?$
ν_7	non-radial mode?	
ν_a	5;-4 or 6;-4?	4.48 ± 0.13
ν_8	2;-1, 2;-2 or 1;-1	6.04 ± 0.03 or 5.60 ± 0.07
ν_9	1;-1 or 2;-1	6.94 ± 0.03
ν_{10}	4;-4	6.27 ± 0.13
ν_b	6;-6, 5;-5 or 4;-4	5.88 ± 0.20 or 6.32 ± 0.16 or 6.77 ± 0.13

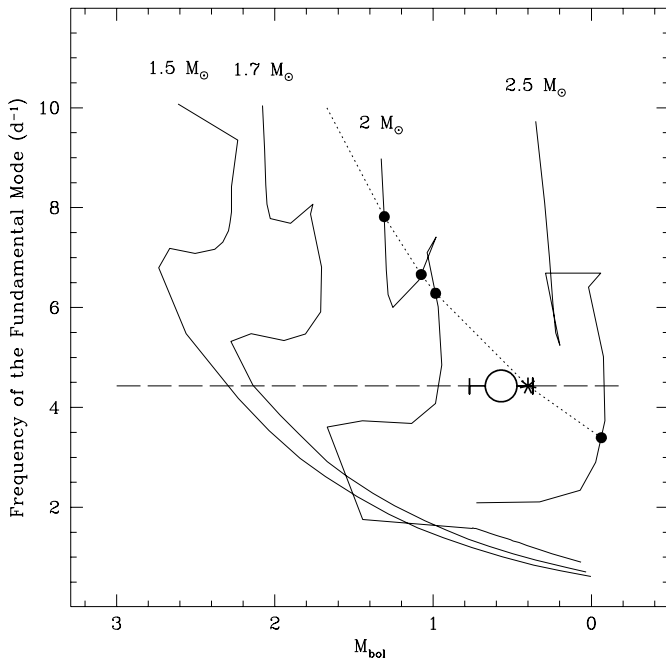


Fig. 9. Evolutionary tracks for different mass values translated into the plane Bolometric Magnitude - Fundamental Frequency (solid lines), the dots indicate the instants of $T_{eff} = 7200^\circ \text{K}$, the horizontal dashed line corresponds to our frequency ν_1 . The representative points of HD 2724 according to the Hipparcos parallax and to our calibration are shown respectively by the open circle with horizontal error bar and by the asterisk.

detected only in the line profile variations deserve a few interesting considerations. The proper Q-value corresponding to ν_a ($0^d.033 \pm 0^d.001$) neither is consistent with a p-mode nor with a g-mode: it would entail the presence in this δ Scuti star of an high ℓ -order f-oscillation. As to ν_b , its most probable de-rotated value seems to show an 1:1 resonance with the observed

Table 4. Basic physical parameters of HD 2724 according to our pulsational model.

Parameter	Estimated value
Mass	$2.25 \pm 0.10 M_\odot$
Effective temperature	$7200 \pm 100^\circ \text{K}$
Absolute bolometric magnitude	$0.4^{+0.2}_{-0.1}$
$\log g$	3.44 ± 0.03
Radius	$4.7 \pm 0.3 R_\odot$
Rotational frequency	$0.46 \pm 0.03 \text{ d}^{-1}$

frequency ν_6 which, therefore, would not need any rotational correction: according to its Q-value of $0^d.025$, we could identify ν_6 as the first radial overtone.

Finally, we have to notice that the pulsational calibration

$$\log g = 2 \log Q\nu - 0.2M_{bol} - 2 \log T_{eff} + 12.908 \quad ,$$

if our hypothesis is correct, permits a particularly accurate gravity determination.

6. Open problems

In this work we could get a few interesting results about the pulsational pattern presented by a δ Scuti star and about its relevance to the study of stellar structure and evolution; nevertheless, we are far from drawing an exhaustive picture of the pulsational behaviour of HD 2724 as well as of other δ Scuti objects.

Our light curves allowed us to detect the presence of at least 10 different periodicities, determining unambiguously no more than 7 frequencies. Apparently, observational bases like our 11 high quality photometric nights at La Silla are inadequate if

faced by the complex variability of these stars. The last instructive example of such complexity is provided by Breger et al. (1998), who identify 24 frequencies in the light curve of FG Vir, discovering, moreover, 8 additional promising candidate pulsational components and finding evidence of considerable amplitude variations (maybe due to beats between unresolved frequencies) affecting one of the detected periodicities in a time scale of one year. In the above mentioned paper, Breger and his collaborators show also the way to obtain this kind of results, which are basically the fruits of the largest photometric multi-site campaign devoted to date to a δ Scuti star.

The inadequacy of our data becomes dramatic on the spectroscopic side. In fact, although the scrutiny of our spectroscopic series led us to discover two additional high ℓ -order non-radial pulsation invisible in the light curves, the poor spectral window of these data did not even allow a reliable determination of the corresponding frequencies. Besides, blending close periodicities who could be photometrically resolved, it affected also the subsequent mode identification. Unfortunately, it is more difficult, even if not less important, to obtain satisfactory series of spectroscopic observations than photometric ones: to the delicate organizational problems of a multi-site campaign, we would have to add the hard work of elbowing our way to adequate telescopes.

We realize that an exhaustive pulsational picture of the δ Scuti stars might become, under these conditions, nothing more than a tantalizing dream. Nevertheless, let us end on an optimistic note: as shown, for example, just in this work, interesting results can be obtained also from incomplete patterns; besides, unexpected theoretical developments might help to simplify our task. Chandrasekhar & Ferrari (1991, 1992), for example, began to explore the exciting possibility of getting selection rules of pulsational modes through the transfer of methods from the quantum field theory to the general-relativistic treatment of non-radial oscillations.

Acknowledgements. We are grateful to L.A. Balona and E. Poretti for their useful suggestions, thanks are due to Dr. Balona also for allowing us to use his LNPROF code.

References

- Balona L.A.: 1987, MNRAS 224, 41.
 Balona L.A.: 1997, private communication.
 Bossi M., Guerrero G., Mantegazza L., Poretti E., Re R.: 1994, Rev. Mex. Astron. Astrofis. 29, 158.
 Breger M.: 1990, Delta Scuti Star Newsl. 2, 13.
 Breger M., Zima W., Handler G., Poretti E., Shobbrook R.R., Nitta A., Prouton O.R., Garrido R., Rodríguez E., Thomassen T.: 1998, A&A 331, 271.
 Canuto V.M., Mazzitelli I.: 1991, ApJ 370, 295.
 Chandrasekhar S., Ferrari V.: 1991, Proc. R. Soc. London, Sez. A 433, 423.
 Chandrasekhar S., Ferrari V.: 1992, Proc. R. Soc. London, Sez. A 437, 133.
 Crawford D.L.: 1979, AJ 84, 1858.
 Díaz-Cordovés J., Claret A., Giménez A.: 1995, A&AS 110, 329.
 Dziembowski W.: 1977, Acta Astron. 27, 203.
 ESA: 1997, *The Hipparcos Catalogue*, SP-1200.
 Fitch W.S.: 1981, ApJ 249, 218.
 Garrido R., García-Lobo E., Rodríguez E.: 1990, A&A 234, 262.
 Hauck B., Mermilliod M.: 1990, A&AS 86, 107.
 Hoffleit D., Jaschek C.: 1982, *The Bright Star Catalogue*, fourth revised edition, Yale University Observatory, New Haven, CT, USA.
 Kennelly E.J., Walker G.A.M., Merryfield W.J.: 1992, ApJ 400, L71.
 Lampens P.: 1992, A&AS 95, 471.
 Mantegazza L., Poretti E., Bossi M.: 1994, A&A 287, 95.
 Mantegazza L., Poretti E., Zerbi F.M.: 1995, A&A 299, 427.
 Mantegazza L., Poretti E.: 1996, A&A 312, 855.
 Mantegazza L.: 1997, A&A 323, 845.
 Mantegazza L., Poretti E., Bossi M., Nuñez N.S., Zerbi F.M.: 1998, *A Half-Century of Stellar Pulsation Interpretations*, P.A. Bradley & J.A. Guzik eds., ASP Conf. Ser. 135, 192.
 Moon T.T., Dworetzky M.M.: 1985, MNRAS 217, 305.
 Poretti E., Zerbi F.M.: 1993, A&A 268, 369.
 Press W.H., Teukolsky S.A., Vetterling W.T., Flannery B.P.: 1992, *Numerical Recipes in FORTRAN*, 2nd Edition, Cambridge University Press, New York, USA.
 Reipurth B.: 1981, Inf. Bull. Variable Stars 2015.
 Roberts D.H., Lehar J., Dreher J.W.: 1987, AJ 93, 698.
 Schaller G., Schaerer D., Meynet G., Maeder A.: 1992, A&AS 96, 269.
 Telting J., Schrijvers C.: 1995, IAU Symp. 176 "Stellar Surface Structure" Poster Proceedings, K.G. Strassmeier ed., Institut für Astronomie der Universität Wien, Wien, Austria, p.35.
 Vanicek P.: 1971, Astrophys. Space Sci. 12, 10.
 Villa P., Breger M.: 1998, private communication.
 Watson R.D.: 1988, Astrophys. Space Sci. 140, 255.